The Technical and Clinical Implementation of LATTICE Radiation Therapy (LRT)

Authors: Wu, Xiaodong, Perez, Naipy C., Zheng, Yi, Li, Xiaobo, Jiang, Liuqing, et al.

Source: Radiation Research, 194(6) : 737-746

Published By: Radiation Research Society

URL: https://doi.org/10.1667/RADE-20-00066.1

RADIATION RESEARCH **194**, 737–746 (2020)
0033-7587/20 $15.00

DOI: 10.1667/RADE-20-00066.1

The Technical and Clinical Implementation of LATTICE Radiation Therapy (LRT)

Xiaodong Wu,[a,b,c,d,1] Naipy C. Perez,[b] Yi Zheng,[a,d] Xiaobo Li,[d] Liuqing Jiang,[d] Beatriz E. Amendola,[b] Benhua Xu,[d] Nina A. Mayr,[e] Jiade J. Lu,[c] Georges F. Hatoum,[f] Hualin Zhang,[g] Sha X. Chang,[h] Robert J. Griffin[i] and Chandan Guha[j]

[a] Executive Medical Physics Associates, North Miami Beach, Florida; [b] Innovative Cancer Institute, South Miami, Florida; [c] Department of Medical Physics, Shanghai Proton and Heavy Ion Center, Fudan University Cancer Hospital, Shanghai Engineering Research Center of Proton and Heavy Ion Radiation Therapy, Shanghai, China; [d] Department of Radiation Oncology, Fujian Medical University Union Hospital, Fuzhou, Fujian, China; [e] Department of Radiation Oncology, University of Washington School of Medline, Seattle, Washington; [f] JFK Comprehensive Cancer Institute, Lake Worth, Florida; [g] Department of Radiation Oncology, Northwestern University Feinberg School of Medicine, Chicago, Illinois; [h] Department of Radiation Oncology, University of North Carolina, Chapel Hill, North Carolina; [i] Department of Radiation Oncology, University of Arkansas for Medical Sciences, Little Rock, Arkansas; and [j] Department of Radiation Oncology Albert Einstein College of Medicine and Montefiore Medical Center, Bronx, New York

Wu, X., Perez, N. C., Zheng, Y., Li, X., Jiang, L., Amendola, B. E., Xu, B., Mayr, N. A., Lu, J., Hatoum, G., Zhang, H., Chang, S. X., Griffin, R. J. and Guha, C. The Technical and Clinical Implementation of LATTICE Radiation Therapy (LRT). *Radiat. Res*. 194, 737–746 (2020).

The concept of spatially fractionated radiation therapy (SFRT) was conceived over 100 years ago, first in the form of GRID, which has been applied to clinical practice since its early inception and continued to the present even with markedly improved instrumentation in radiation therapy. LATTICE radiation therapy (LRT) was introduced in 2010 as a conceptual 3D extension of GRID therapy with several uniquely different features. Since 2014, when the first patient was treated, over 150 patients with bulky tumors worldwide have received LRT. Through a brief review of the basic principles and the analysis of the collective clinical experience, a set of technical recommendations and guidelines are proposed for the clinical implementation of LRT. It is to be recognized that the current clinical practice of SFRT (GRID or LRT) is still largely based on the heuristic principles. With advancements in basic biological research and the anticipated clinical trials to systemically assess the efficacy and risk, progressively robust optimizations of the technical parameters are essential for the broader application of SFRT in clinical practice.

INTRODUCTION

Since its early inception over 100 years ago by Kohler (*1–4*), spatially fractionated radiation therapy (SFRT) in the form of 2D GRID has been applied clinically, although not as a mainstream radiation therapy modality. While conducting systemic clinical trials has been practically difficult, the reported clinical data have suggested favorable outcomes and clinical value of GRID therapy for the treatment of advanced bulky tumors (*5–16*). A recent workshop sponsored by the National Cancer Institute (NCI) and Radiosurgery Society (RSS) for assessment of, and discussion on, the techniques and clinical merits of SFRT resulted in a comprehensive summary report (*6*). The physical 2D GRID blocks or apertures, evolving from the early kV X-ray delivery systems to the modern-day megavoltage accelerators, with the same intention of normal tissue sparing, generate similar patterns of peak-to-valley dose distribution. Over the years, a consensus has been gradually established among the relatively small community of GRID practitioners regarding the GRID dose distribution and the methods of treatment delivery (*17, 18*). In addition to a number of published reviews (*6–10*), an article published in this special issue by Zhang *et al*. updates the collective understanding and technical perspectives on GRID radiation therapy.

It was proposed in 2010 that the 2D GRID could be extended to a 3D configuration, in which an array of high-dose regions (vertices) could be created within the tumor volume through converging photon beams or by the Bragg peaks of charged particle beams (*19*). The high-dose vertices are separated by a certain distance to give rise to the peak-to-valley dose distribution. Such technical approach is referred to as LATTICE radiation therapy (LRT) (Fig. 1).

The GRID was originally introduced with the objective of sparing normal tissues, especially the skin, in the kilovoltage (KV) and 2D imaging era of radiation therapy (*1–5*). As the newer biological data suggested possible bystander and abscopal effects (*20–27*), the unique peak-to-valley dose distribution of GRID has been postulated to

Editor's note. The online version of this article (DOI: https://doi.org/10.1667/RADE-20-00066.1) contains supplementary information that is available to all authorized users.

[1] Address for correspondence: Executive Medical Physics Associates, 19470 NE 22nd Road, North Miami Beach, FL 33179; email: drxiaodongwu@yahoo.com.

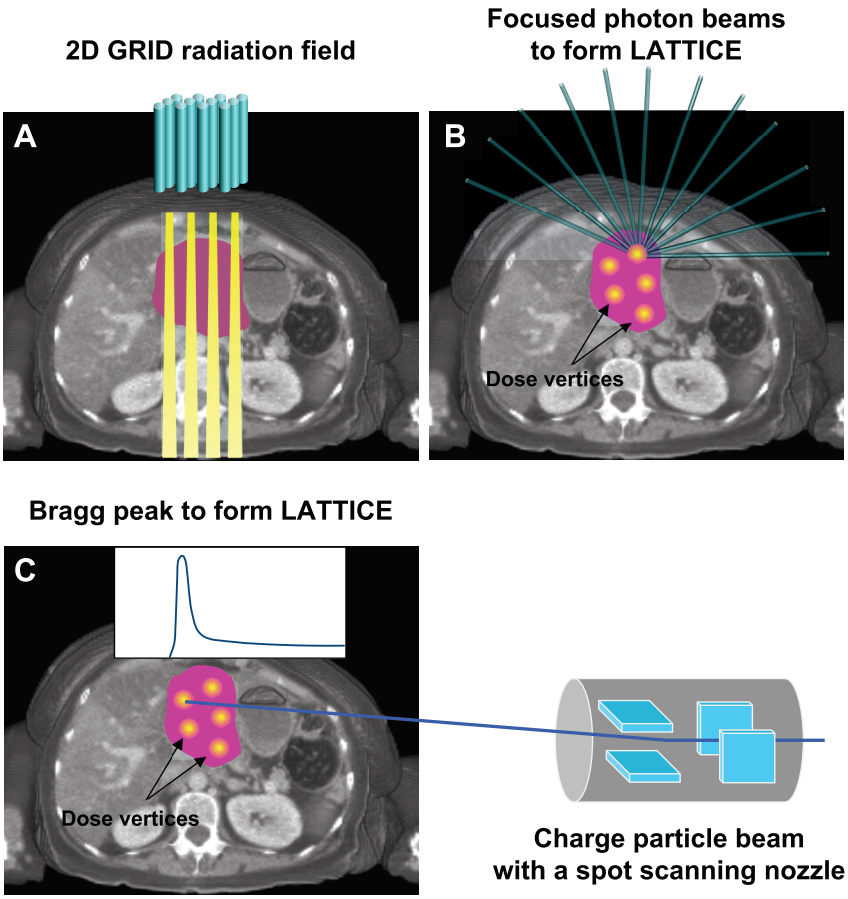

FIG. 1. LATTICE radiation therapy as a 3D extension of GRID. Panel A: 2D GRID. Panel B: 3D LATTICE with focused photon beams. Panel C: 3D LATTICE with charged particle beams

be the key contributor to such effects. Introduced as a 3D extension of GRID in the modern era of radiation therapy, LRT offers additional flexibility to achieve the goals of SFRT. When leveraging intensity modulated radiation therapy (IMRT)/volumetric modulated arc therapy (VMAT) and image guiding capabilities, with 3D LRT, not only can one achieves better skin and normal tissue sparing, but also generate highly customized peak-to-valley dose distribution within the tumor volume to achieve the intended safe partial radiation ablation or to mediate as postulated, bystander and abscopal effects, such as anti-tumor immunity.

Importantly, LRT has physical features that are uniquely different from the traditional GRID therapy. The similarities between the two are more historical rather than mechanistic. As such, the cumulated clinical experience of GRID could not be directly applied to LRT.

Based on the key objectives of delivering a high dose of radiation to a large tumor with minimized toxicity and forming peak-to-valley dose distribution within the tumor volume, pending systemically proven clinical efficacies by randomized clinical trials, there could be two types of clinical applications with LRT.

One application can be used to safely deliver high-dose to partial volume of advanced large tumors without causing excessive toxicities, and for the purpose of palliative tumor debulking or boost treatment. With such intent, LRT can be administered alone or combined with conventionally fractionated radiation therapy.

Another application would be for certain types of tumors that exhibit responses differentially to radiation doses through mechanisms such as immunomodulation (*28*). Here, LRT might be used to promote bystander and abscopal effects with the intent to improve tumor local control and systemic therapeutic outcome through, for example, induced anti-tumor immunity. Although radiation-induced immunogenicity has been observed, to augment such effect sufficiently to achieve meaningful improvement of therapeutic outcome is not trivial, as radiation therapy can lead to both immune activation (*29*) and immune suppression (*30*). It has been shown in both pre-clinical and clinical studies that either a single-fraction or hypofractionated (2–5 fractions) ablative dose of radiation, such as in stereotactic radiosurgery (SRS) and stereotactic body radiotherapy (SBRT), can induce anti-tumor T-cell immunity and lead to effective tumor local control and even systemic therapeutic effects (*28–41*). However, it has been recognized that ablative dose could also exhibit several immunosuppressive features (*42*) and reduce tumor perfu-

sion (*43, 44*), which could counter the induced anti-tumor immunity. On the other hand, it has been shown that low-dose radiotherapy is capable of reprogramming the immunosuppressive tumor microenvironment (TME) to become more immunogenic (*45–47*) and could also improve perfusion (*49, 50*). Although conventional fractionated radiotherapy has been shown to be counterproductive if given as an adjuvant treatment to immunogenic ablative radiotherapy (*28*), sequential arrangement of a single fraction of ablative dose followed by limited fractions of low-dose radiation (post-ablation modulation) has been shown effective in amplifying anti-tumor immunity in preclinical studies (*48*). All these suggest the crucial importance of choosing dose and fractionation scheme and the appropriate target cells in order to harvest the widest range of anti-tumor effects to achieve optimal treatment outcome (*41*).

In light of the sequential or temporal arrangement of single ablative dose with low dose post-ablation modulation (*48*), the peak-to-valley dose distribution of SFRT could be viewed, in essence, as a spatial arrangement/distribution of high and low doses that might synergistically augment the anti-tumor immunity. In this context, an ideal peak-to-valley configuration should have the peak dose sufficiently high to induce tumor-specific immunogenic response, and the valley dose sufficiently low (<5 Gy) to preserve tumor microvasculature and perfusion to allow for circulation of cytokines/chemokines and/or immunogenic factors (*45, 49–53*) and to synergize the induced anti-tumor immunity. Logically, with such intent (immune activation), adjuvant conventional radiotherapy will not be desirable, as the prolonged fractionated treatments will have the potential to deplete activated T cells (*28, 41*); rather, combined treatment with enhancement of tumor antigen presentation and/or immune checkpoint blockades should be favorable (*15, 31, 36–38, 54–56*).

Depending on the treatment objectives (partial debulking/boost, or induction of anti-tumor immunity), factors or parameters potentially contributing to the therapeutic effectiveness of SFRT would include the geometric configuration (peak-to-valley distribution), differential dose level, and the combination of other treatment modalities such as conventional radiotherapy, low-dose irradiation (await for clinical trials) and immunotherapy (*8–10, 15, 31, 48, 54–56*).

Recognizing the difficulties of translating animal data of small scale (mm range) to clinical settings, currently the physical/dosimetric parameters of clinical SFRT are still largely based on the traditional configuration dating back to the early era of GRID, namely the dimensions of peaks and valleys are in the order of 1 cm. Similarly, LRT has been using a comparable dimensional magnitude: the dose vertices consist of sphere-like high-dose sub-volumes (vertices) with diameters of approximately 1 cm, with the separation between dose vertices of approximately 2–5 cm (center to center). Following this approach, the placement of vertices (LATTICE layout) is iterated during planning until the dose criteria are met, using essentially the IMRT/VMAT dose-painting technique or IMPT (intensity modulated particle therapy). As a general rule, the dose to the tumor periphery is kept to a level deemed tolerable by the surrounding normal tissues and critical organs.

Quantitative assessment for biological response is currently limited. With the intent of palliative partial treatment, the tumor response is likely to follow the traditional radiobiological prediction by parameters such as the effective uniform dose (EUD) (*57, 58*). For the intent of inducing anti-tumor immunity, the biological models are limited, and it is important for the novel development to include the interactions between different subunits of a tumor and the systemic effects, to guide the clinical trials to provide rigorous proof of clinical efficacy and an understanding of potential toxicities.

The purpose of this article is to recap the physics of LATTICE radiation therapy and to present a set of dosimetric guidelines based on the limited clinical experience accumulated up until now, which are provisional by nature, intended to provide a certain level of technical uniformity and safety for delivering LRT. The standardization and prospective exploration of putative parameters, informed by laboratory and clinical data, will be essential for the appropriate application and understanding before wider acceptance of LRT if/as indicated.

CLINICAL APPLICATION

Since its early introduction in 2010 (*19*), over 150 patients with late-stage bulky tumors have received LRT, mainly in two centers, at the Innovative Cancer Institute (Miami, FL) and at the Fujian Union Hospital (Fuzhou, China). The LRTs were applied either alone or in combination with conventionally fractionated radiotherapy, chemotherapy or immunotherapy. Responses to LRT varied depending on clinical conditions. The clinical outcomes have been published in small series and several consecutive case reports (*59–63*). A number of retrospective reviews with statistics are in the preparatory stage of publication.

The Innovative Cancer Institute reported 56 cases treated with LRT alone ($n = 8$) or in combination with conventional radiotherapy and/or chemotherapy (86%), from April 2010 to July 2019, in various body sites (Table 1). The tumor types included lung, gynecological, renal cell, head and neck, sarcoma, colon, anal and skin. The tumor sizes ranged from 40.5–1,494.9 cc. The LRT vertex dose ranged from 2.4–18.0 Gy per fraction.

The Department of Radiation Oncology at the Fujian Union Hospital reported 69 cases treated with LRT alone ($n = 34$) or in combination with conventional radiotherapy, chemotherapy and/or immunotherapy (51%), from April 2017 to December 2019 (Table 2). The tumor types included lung, breast, thymoma, liver, gynecological, upper GI, chordoma, lymphoma, renal cell, head and neck, sarcoma, colon, anal and skin. The tumor sizes ranged

TABLE 1
LATTICE Treatment Case Statistics: Innovative Cancer Institute, South Miami, FL, April 2010–July 2019

Site	No. of patients	GTVmin (cc)	GTVmax (cc)	Average vertice diameter (cm)	V_V/V_{GTV} (%)	Fractional dose (Gy)		No. of cases treated with LATTICE alone
						Median vertices	Min/max vertices	
Pelvis	20	74.1	1,000.1	1.1	1.8	8	2.4/15	1 (3 fx)
Lung	18	45.9	680.4	1.1	1.3	18	4.5/18	2 (5 fx)
Retroperitoneum	7	114.6	866.1	1.4	2.3	12	10/16	4 (1–5 fx)
Head and neck	5	59.6	196.7	1.2	2.2	10	10/15	0
Extremities	3	137.3	688.5	1.5	1.9	5.8	5.3/11.8	0
Abdomen	2	95.0	1,494.9	1.3	2.6	9	9/9	0
Mediastinum	1	40.5	40.5	0.8	7.2	8	8/8	1 (1 fx)

from 17.4–3,784.1 cc. The LRT vertex dose ranged from 8.0–20.0 Gy per fraction.

In the presented list, the majority of cases received LRT with palliative intent as partial ablative tumor debulking or as boost treatment. As an example of this type of application, in one of their case reports (*61*), Amendola *et al*. described the successful treatment using LRT combined with conventional radiotherapy for a stage IIIA NSCLC of 218.5 cc. For this tumor, the LRT consisted of three high-dose vertices with 18 Gy of peak dose and less than 3 Gy of tumor peripheral dose, delivered using the VMAT technique. In the subsequent conventional radiotherapy, 2 Gy × 29 fractions were delivered to the planning target volume (PTV). The tumor steadily regressed after the treatment and the patient is currently status ''no evidence of disease'' (NED), 9 years after the treatment. Figure 2 shows the LRT dose distribution and the tumor response 15 months after the completion of total treatment.

For the cohort of patients who were indicated for immunotherapy, the second type of LRT application was given to some patients with the intent of inducing anti-tumor immunity, in combination with immune checkpoint blockade treatment. Some of the tumors in this group were not particularly bulky in the conventional sense, but were relatively large by the common standard of SRS or SBRT. Benhua Xu *et al*. reported a case of a metastatic NSCLC tumor of 63.2 cc.[2] The tumor cells had 70% expression of PD-L1. The patient received a single fraction of LRT with 20 Gy prescribed to six high-dose vertices using a Cyberknife robotic radiosurgery system, combined with anti-PD-1 immunotherapy. The minimal valley dose was 2.9 Gy with 30% of the GTV receiving 5 Gy or less. The mass regressed 78% over one month after LRT and achieved complete local tumor response five months after LRT (Fig. 3). A case report with the full details has been submitted for publication and is currently under review.

Pollack *et al*. recently reported the results of a phase I clinical trial using LRT as an upfront boost followed by standard fractionation radiotherapy for prostate cancer (*63*). Twenty-five patients with favorable-to-high-risk prostate cancer were enrolled and treated. The LATTICE boost plan consisted of 1–3 cylindrical-shaped vertices identified by multiparametric MRI as suspicious gross tumor volumes within the prostate gland. The vertices were treated on day 1 with 12 Gy. The entire prostate, along with the proximal seminal vesicles, was then treated with definitive standard fractionation radiotherapy. No unexpected toxicity was observed with the median follow-up of 66 months. Note that the use of the LATTICE technique in this study is different from the majority of the historically treated LRT cases, in the sense that the prostate gland is not considered as a bulky solid tumor. Having the objective to improve disease control by using LRT as a boost, this phase I study was set to examine the feasibility and safety of the approach and has now laid the foundation for a follow-up phase II randomized trial.

[2] Personal communication.

TABLE 2
LATTICE Treatment Case Statistics: Fujian Union Hospital, Fuzhou, China, April 2017–December 2019

Site	No. of patients	GTVmin (cc)	GTVmax (cc)	Average vertice diameter (cm)	V_V/V_{GTV} (%)	Fractional dose (Gy)		No. of cases treated with LATTICE alone
						Median vertices	Min/max vertices	
Chest	21	63.2	3,784.1	0.91	1.8	15.0	8/20	10 (1–3 fx)
Abdomen	16	17.4	1,118.6	0.92	2.1	15.0	10/20	7 (1–2 fx)
Head and neck	11	21.4	368.4	0.87	2.2	15.0	8/15	4 (1–2 fx)
Lung	11	41.1	3,034.4	0.95	1.6	15.0	10/18	6 (1–3 fx)
Spine	4	57.9	510.3	0.85	2.1	15.0	12/20	3 (2–3 fx)
Extremities	3	154.3	2,072.9	0.87	1.5	15.0	15/18	2 (1–2 fx)
Pelvis	3	131.6	777.9	0.87	1.2	15.0	10/20	2 (2 fx)

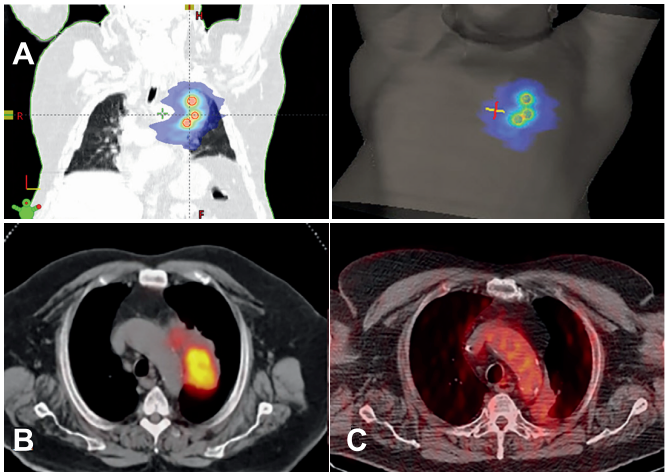

FIG. 2. LRT for a stage IIIA lung tumor as upfront boost (*61*): 18 Gy to the vertices, 3 Gy to the periphery of the PTV. Panel A (top row): Dose distribution. Panel B: Tumor prior to treatment. Panel C: Follow-up PET-CT 15 months after LRT followed by 2 Gy × 29 fractions of VMAT.

PHYSICS AND DOSIMETRY

Generally, a photon delivery system that is commissioned for SRS/SBRT is considered suitable for delivering LRT (*19, 59–63*). There is no special requirement for additional beam acquisition or modeling beyond that for SRS/SBRT. This section focuses on the treatment planning parameters, plan evaluation, treatment delivery and data reporting.

Treatment Planning Parameters

To date, all LRT treatments were delivered by either IMRT/VMAT using a conventional linear accelerator (linac) or the Cyberknife system. Particle-based LRT is in the experimental stages. Figure 4 shows the recommended geometric and dosimetric parameters used for a typical LRT plan. The first step in LRT planning is to determine a LATTICE layout, according to which high-dose vertices with each a sphere of 0.5–1.5 cm in diameter are created and distributed within the gross tumor volume (GTV) with separation of 2.0–5.0 cm from each other (center-to-center). Intra-fractional motion should also be taken into consideration in fine-tuning the vertex size. To avoid excessive dose to the surrounding normal tissues, a LATTICE inward margin (1–2 cm) is often introduced to keep the vertices at a certain distance from the tumor boundary. To effectively control and assess the LRT dose distribution, a LATTICE volume (V_L) is created by connecting the outer-most vertices or by contracting the GTV by the LATTICE inward margin. There is no rigorous requirement for the symmetry of placing high-dose vertices, or for the uniformity of their size or shapes. The total number of high-dose vertices depends on the size and the shape of the tumor volume, as well as the resolution of beam apertures, for example, the MLC width and the diameters of collimating cones. A system of estimating the number of high-dose vertices based on tumor volume, vertices separation and LATTICE inward margin is provided in the LRT worksheet (Supplementary Information; https://doi.

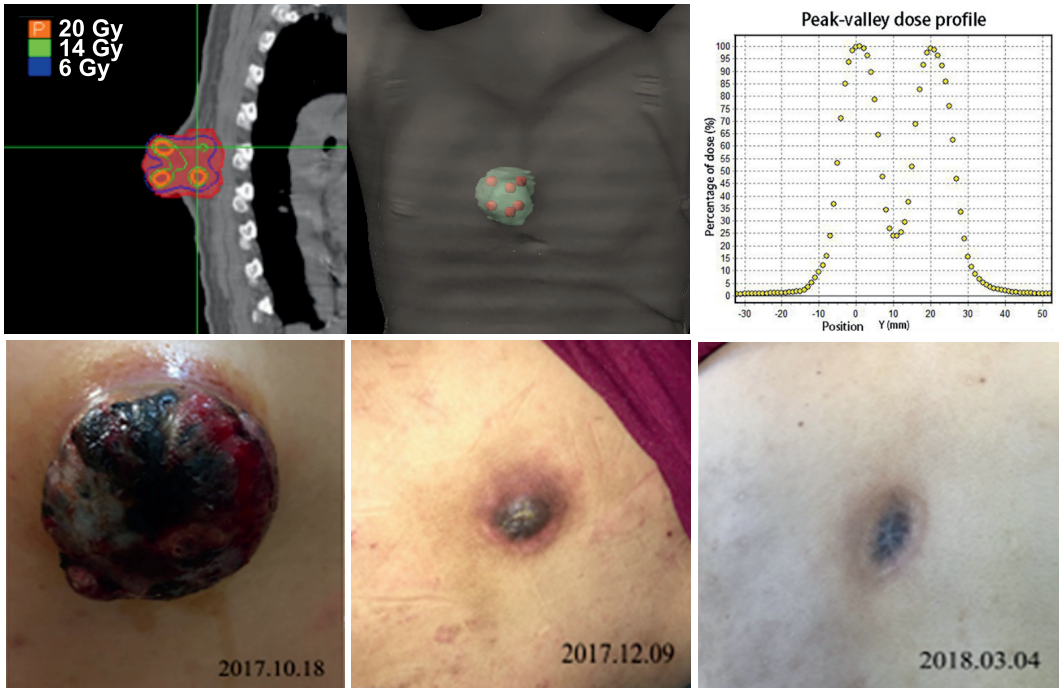

FIG. 3. Single LRT for a lung metastasis. Top row: Dose distribution. Bottom row: Pre- and postirradiation tumor regressions.

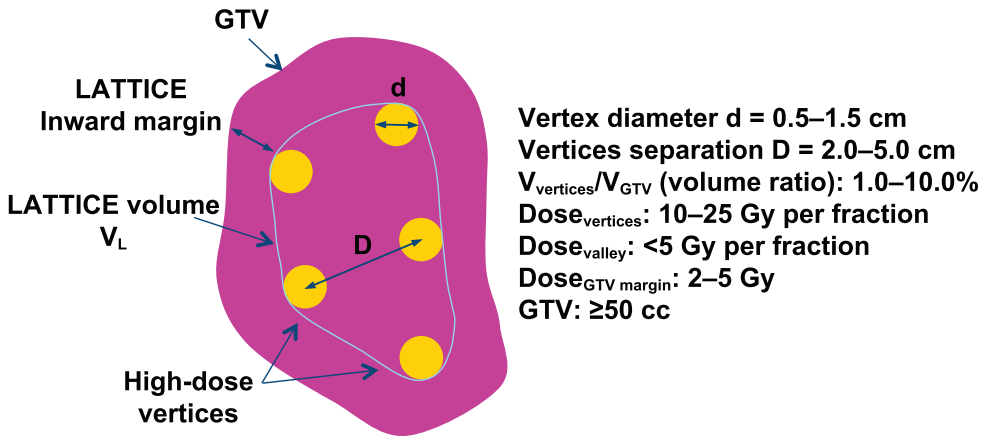

FIG. 4. Parameters and ranges of a typical LRT plan.

org/10.1667/RADE-20-00066.1.S1). Depending on the actual tumor shape and specific needs, such as avoiding nerves and blood vessels in the tumor, the actual number of vertices could be more or much less. The planning parameters can also vary depending on the radiation delivery methods, i.e., gantry-mounted linac or robotic non-isocentric system. In determining the LATTICE layout, mainly GTV is taken into account. Clinical target volume (CTV) or internal target volume (ITV) and planning target volume (PTV) are included in LRT planning for the purpose of peripheral dose control and for the integrated consideration with other combined radiotherapy modalities.

The prescription of an LRT plan requires specifications of peak dose, valley dose and tumor peripheral dose. The peak dose is prescribed to cover 95% of the high-dose vertices and valley dose is the minimal dose within the LATTICE volume (V_L); target peripheral dose specifies the maximum allowable dose around the tumor margin for the purpose of toxicity control (typically <3Gy). In general, it is favorable to have as wide as possible difference between peak and valley doses (50–80%). Additional criteria might be required depending on the intent of LRT. For palliative or boost treatment, the peak dose could have a wider range, for example 5–20 Gy, and the value of valley dose is not crucial, as long as toxicity control can be assured. For induction of anti-tumor immunity, the peak dose is recommended to be 15–25 Gy (or higher), with the valley dose less than 5 Gy (or as low as reasonably achievable), based on the rationales given in the introduction. With the current photon beam technologies, the ability to lower valley dose might be limited, whereas charged particle beam may overcome this limitation.

Due to the intrinsic configuration different from GRID, the valley-to-peak dose ratio (VPDR) for LRT is recommended as the ratio of Dmean(95–100) of the LATTICE volume (V_L) to the prescribed peak dose Dp, i.e., Dmean(95–100)/Dp, where Dmean(95–10), the mean dose of the 5% of V_L that receives the lowest range of doses, can be derived from the dose-volume histogram (DVH) of the LATTICE volume (V_L) from 100% to 95% volume coverage.

Once the LATTICE layout and dose-volume objectives are determined, inverse planning can be initiated. Because the optimization algorithms in current treatment planning systems (TPS) are not tailored to LRT, multiple iterations (to adjust LATTICE Layout and dose-volume objectives) are generally needed to obtain the desired LRT dose distribution. As shown *in* Tables 1 and 2, in the resulting LRT plans the total volume of vertices receiving the prescribed peak dose ranged from 1% to 10% of the GTV volume, with the most frequent value at approximately 2%.

As an example, for a GTV of 225 cm^3 with the total volume of all vertices at 2% of the GTV, i.e., 4.5 cm^3, assuming the diameter of a vertex to be 1.0 cm (0.52 cm^3), the total number of vertices is then calculated to be 8.6. With a relatively round tumor, 7–9 vertices with approximately 3 cm of vertices separation can be anticipated for this tumor. However, if the tumor has an elongated shape and is adjacent to certain critical structure(s), the number of vertices could be reduced to 5 with vertex diameter of 1.2 cm and separation of approximately 4 cm.

Additional caution should be exercised to avoid placing high-dose vertices on or close to the neural structures, large vessels and bones that are often found entangled within bulky tumors.

Treatment Delivery

As stated earlier, the technical requirements of LRT can be best equated to that of SRS/SBRT. Stereotactic setup is highly recommended to ensure accurate delivery of LRT, which implies precise image guidance, and respiratory motion management if indicated. The robustness in patient setup and immobilization is essential, not so much because of the concern for normal tissue toxicity outside of the tumor, but the potential blurring effect of vertices dose and the possible presence of critical structures inside the tumor volume.

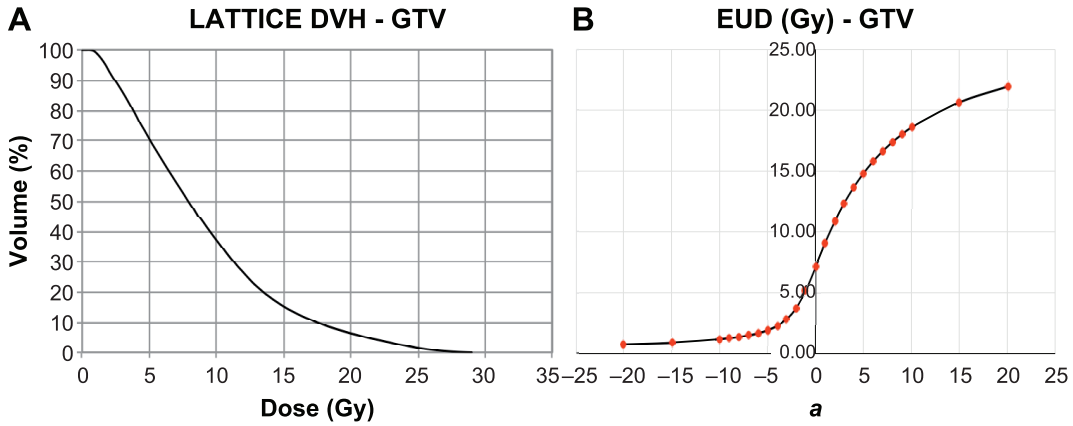

FIG. 5. Panel A: DVH of the GTV in the second clinical example. Panel B: The associated EUD as a function of biological sensitivity scaling factor a.

Patient-specific QA for LRT plans should follow standard IMRT/VMAT-based SRS/SBRT QA protocols/procedures, using equipment such as portal dosimetry, film and/or high-resolution diode array-based QA systems.

Dose-Volume Characteristic and Analysis

LRT intentionally delivers highly heterogeneous dose distribution to large tumors, resulting in its signature DVH pattern that is markedly different from conventional external beam radiation therapy, but resembles low- or high-dose-rate interstitial brachytherapy. As an example, Fig. 5A shows the DVH of the tumor mass from the previously described example of combined LRT with anti-PD-1 immunotherapy (second clinical example). Only 6.5% of the GTV received the prescribed LRT dose of 20 Gy, while 30% of the GTV received a dose below 5 Gy.

In evaluating the quality of a treatment plan, the concept of EUD has been frequently used to predict the effectiveness of tumor control and normal tissue toxicity. One form of EUD was suggested by Niemierko as (*57, 58*):

$$EUD_a = \left[\sum_i (v_i D_i^a)\right]^{1/a},$$

where v_i is the fraction of the ith sub-volume receiving dose D_i, and a is a scaling factor that is unique to the tissue's characteristics and radiation sensitivity. Traditionally, tumors will assume a large negative value of $\boldsymbol{a}$ (e.g., –10), while normal tissues will assume a positive number with serial architecture having relatively larger value (e.g., +10). Although EUD has also been used as one of the characteristic parameters in reporting GRID radiotherapy, its interpretation remains unclear. Following conventional radiobiological principles, failure of tumor control is highly susceptible to ''missing the target'' or under-coverage of tumor volume by the prescribed dose. Therefore, with a large negative value of $\boldsymbol{a}$, EUD will lean toward the minimal tumor dose, and would apply more fittingly to the first category of LRT application for palliative partial debulking or boost treatment.

Reflecting on the long-standing clinical experience with SFRT, an EUD calculated with $\boldsymbol{a} = -10$ would not have predicted many of the reported clinical outcomes. The EUD calculated from the DVH of Fig. 5A, as a function of $\boldsymbol{a}$, is shown in Fig. 5B, in which $EUD_{-10} = 1.2$ Gy, suggesting a negligibly low rate of tumor control, while $EUD_{+10} = 18.6$ Gy, suggesting a high rate of tumor control that is apparently better correlated to the clinical observation of this particular example. This further suggests that the physical configuration of SFRT and other unconventional biological mechanisms, such as immunogenic effects, could affect the value of $\boldsymbol{a}$. As such, this EUD formulism with a single coefficient may offer a means to incorporate other SFRT-induced effects. The effective $\boldsymbol{a}$ value could, in principle, be obtained by comparing iso-tumor responses between SFRT and series of uniform irradiations.

As LRT dose distributions are vulnerable to motion due to the nature of high dose gradient, EUD could also be used to evaluate the robustness of a LRT plan in terms of the impact of tumor motion on biological effects.

Reporting LRT Plan

To report a LRT plan, the following data should be included: treatment objective; combined treatment modalities; GTV; CTV/ITV; PTV; size of high-dose vertex; vertices separation (center to center); number of vertices; total volume of the vertices; LATTICE volume (V_L); vertices-GTV volume ratio; peak dose prescribed to the vertices (Dp) and the maximum vertex dose (Dmax); minimal dose between the vertices (valley dose); DVHs of the total vertices, GTV, CTV/ITV, PTV, V_L and all relevant critical structures; VPDR defined as Dmean(95–100)/Dp of V_L; and $EUD_{a=-10}$ of the GTV. The worksheet (Supplementary Information; https://doi.org/10.1667/RADE-20-00066.1.S1) aims to assist the LRT planning and data reporting.

CONCLUSION AND DISCUSSION

SFRT takes on a number of forms: GRID, LATTICE, micro-beam and mini-beam (*8–10, 13, 64–66*). Following a long history of clinical practice of GRID, LRT has cautiously entered the field. From the relatively small collection of LRT clinical cases, no adverse radiation-treatment-related toxicity has been observed or reported; high tumor responses, similar to that of GRID therapy, have been reported and the technical feasibility of LRT has been demonstrated.

Strongly grounded in the experience of GRID therapy, beam configurations in LRT (depending on the delivery system) are based on the objective of producing the peak-to-valley dose distribution to achieve a similar clinical response as GRID, but with the added flexibility of individualized 3D configurations without the requirement of rigorous symmetry. The unique features of enclosing high-dose vertices within tumor volume while keeping tumor periphery at the level of conventional fractionation dose further ease the toxicity concern and make LRT inherently more advantageous in delivering SFRT to deep-seated bulky tumors. The flexibility of LRT further includes the option of placing high-dose vertices in the regions of biological significance guided by functional imaging (*63, 67*).

The size of vertices may be influenced by the clinically available instrumentations. A vertex size of 0.5–1.5 cm has been shown to be practically achievable. Larger vertex sizes are possible but might be limited by the dose gradient needed to assure the sufficiently low valley dose.

As treatment intentions may vary, each LRT plan should be carefully individualized. Currently, the most established uses of LRT are for palliation or for boost treatment. Both physical principles and early clinical experience have shown the feasibility and safety of such LRT applications. The classical radiobiological mechanism of DNA double-strand breaks provides a sound base to predict the clinical efficacy. Ablative irradiation to partial tumor volume is essentially tumor debulking, and any additional dose that can be safely delivered to any part of the tumor (boost) should result in greater tumor cell death. To achieve such objectives, the guidelines of this article can offer straightforward and effective assistance.

The use of LRT to mediate bystander and abscopal effects is continuously under active investigation. The recently discovered mechanism of tumor cure using high-dose irradiation, through ceramide-mediated ischemia/reperfusion injury, with preclinical data (*68*) and clinical evidence (*69*) lends further support to this approach. The justification for the general clinical implementation involves many factors, including the combined treatment modalities with optimal sequence to augment bystander and abscopal effects, which have yet to be further explored and evaluated with the clinical efficacy being systemically proven. The guidelines of this article can, at minimum, provide a safe framework for clinical studies or for delivering LRT to a selective group of patients who are medically excluded from receiving any other currently proven treatment modalities.

Criteria used to effectively evaluate SFRT plans need further development. Biological effects beyond DNA double-strand breaks should be incorporated into the development of a more general biophysical model, informed by well-conducted laboratory and clinical studies and correlative science, to guide the future optimization of SFRT planning and delivery.

The guidelines, recommendations and parameters presented in this article are derived from the limited clinical LRT experience, and are of provisional nature. As pointed out by Coleman and Ahmed in an editorial article (*70*) following the NCI and RSS sponsored workshop: ''...we emphasize that medical treatments that are technically feasible are not necessarily clinically indicated...''. Rigorous clinical studies are imperative to advance the experience from the small SFRT community to systemic proof. Until such time, for each patient to be considered for SFRT, the merits and risks must be strictly, individually justified.

SUPPLEMENTARY INFORMATION

LRT Worksheet. This worksheet was developed for the purpose of assisting LRT planning with provisional premise. The estimate of LATTICE number is based on the cylindrical model of GTV. A set of the coefficients k and m are given and recommended for several different volume groups. For each group, the user should not apply a GTV volume smaller than the lower limit. The digital form can be obtained from the corresponding author.

ACKNOWLEDGMENTS

We thank Dr. Mansoor M. Ahmed for his inspiration and key contribution to the development of LATTICE radiation therapy, and his guidance in the preparation of this article. XW is the co-inventor of U.S. Patent No. 8,395,131: Method of 3D Lattice Radiotherapy.

Received: March 1, 2020; accepted: August 24, 2020; published online: October 16, 2020

REFERENCES

1. Liberson F. The value of a multi-perforated screen in deep X-ray therapy. Radiology 1933; 30:186–95.
2. Marks H. A new approach to the roentgen therapy of cancer with the use of a grid. J Mt Sinai Hosp N Y 1950; 17:46–8.
3. Marks H. Clinical experience with irradiation through a grid. Radiology 1952; 58:338–42.
4. Laissue JA, Blattmann H, Slatkin DN. Alban Kohler (1874–1947): Inventor of grid therapy. (Article in German) Z Med Phys. 2012; 22:90–9.
5. Freid JR, Lipman A, Jacobson LE. Roentgen therapy through a grid for advanced carcinoma. Am J Roentgenol Radium Ther Nucl Med 1953; 70:460–76.
6. Griffin RJ, Ahmed MM, Amendola B, Belyakov O, Bentzen SM, Butterworth KT, et al. Understanding high-dose, ultra-high dose

rate, and spatially fractionated radiation therapy. Int J Radiat Oncol Biol Phys 2020; 107:766–78.

7. Mohiuddin M, Curtis DL, Grizos WT, Komarnicky L. Palliative treatment of advanced cancer using multiple nonconfluent pencil beam radiation. A pilot study. Cancer 1990; 66:114–8.
8. Mohiuddin M, Stevens JH, Reiff JE, Huq MS, Suntharahgam N. Spatially fractionated (GRID) radiation for palliative treatment of advanced cancer. Radiat Oncol Investig 1996; 4:41–7.
9. Mohiuddin M, Fujita M, Regine WF, Megooni AS, Ibbott GS, Ahmed MM. High-dose spatially-fractionated radiation (GRID): a new paradigm in the management of advanced cancers. Int J Radiat Oncol Biol Phys 1999; 45:721–7.
10. Penagaricano JA, Griffin R, P. C, Moros E, Yan Y, Ratanatharathorn V. Spatially fractionated (GRID) therapy for large and bulky tumors. J Ark Med Soc 2009; 105:263–5.
11. Kudrimoti M, Regine WF, Huhn JL, Meigooni AS, Ahmed M, Mohiuddin M. Spatially fractionated radiation therapy (SFR) in the palliation of large bulky (>8 cm) melanomas (abstr). Int J Radiat Oncol Biol Phys 2002; 54:342–3.
12. Huhn JL, Regine WF, Valentino JP, Meigooni AS, Kudrimoti M, Mohiuddin M. Spatially fractionated GRID radiation treatment of advanced neck disease associated with head and neck cancer. Technol Cancer Res Treat 2006; 5:607–12.
13. Penagaricano JA, Moros EG, Ratanatharathorn V, Yan Y, Corry P. Evaluation of spatially fractionated radiotherapy (GRID) and definitive chemoradiotherapy with curative intent for locally advanced squamous cell carcinoma of the head and neck: initial response rates and toxicity. Int J Radiat Oncol Biol Phys 2010; 76:1369–75.
14. Neuner G, Mohiuddin MM, Vander Walde N, Goloubeva O, Ha J, Yu CX, et al. High-dose spatially fractionated GRID radiation therapy (SFGRT): a comparison of treatment outcomes with Cerrobend vs. MLC SFGRT. Int J Radiat Oncol Biol Phys 2012; 82:1642–9.
15. Mohiuddin M, Park H, Hallmeyer S, Richards J. High-dose radiation as a dramatic, immunological primer in locally advanced melanoma. Cureus 2015; 7:e417.
16. Zhang H, Wang JZ, Mayr N, Kong X, Yuan J, Gupta N, et al. Fractionated grid therapy in treating cervical cancers: conventional fractionation or hypofractionation? Int J Radiat Oncol Biol Phys 2008; 70:280–8.
17. Meigooni AS, Dou K, Meigooni NJ, Gnaster M, Awan S, Dini S, et al. Dosimetric characteristics of a newly designed grid block for megavoltage photon radiation and its therapeutic advantage using a linear quadratic model. Med Phys 2006; 33:3165–73.
18. Jin JY, Zhao B, Kaminski JM, Wen N, Huang Y, Vender J, et al. A MLC-based inversely optimized 3D spatially fractionated grid radiotherapy technique. Radiother Oncol 2015; 117:483–6.
19. Wu X, Ahmed MM, Wright J, Gupta S, Pollack A. On modern technical approaches of three-dimensional high-dose Lattice radiotherapy (LRT). Cureus 2010; 2.
20. Sathishkumar S, Dey S, Meigooni AS, Regine WF, Kudrimoti MS, Ahmed MM, et al. The impact of TNF-alpha induction on therapeutic efficacy following high dose spatially fractionated (GRID) radiation. Technol Cancer Res Treat 2002; 1:141–7.
21. Sathishkumar S, Boyanovsky B, Karakashian AA, Rozenova K, Giltiay NV, Kudrimoti M, et al. Elevated sphingomyelinase activity and ceramide concentration in serum of patients undergoing high dose spatially fractionated radiation treatment: implications for endothelial apoptosis. Cancer Biol Ther 2005; 4:979–86.
22. Peters ME, Shareef MM, Gupta S, Zagurovskaya-Sultanov M, Kadhim M, Mohiuddin M, et al. Potential utilization of bystander/abscopal-mediated signal transduction events in the treatment of solid tumors. Curr Signal Transduct Ther 2007; 2:129–43.
23. Shareef MM, Cui N, Burikhanov R, Gupta S, Satishkumar S, Shajahan S, et al. Role of tumor necrosis factor-alpha and TRAIL in high-dose radiation-induced bystander signaling in lung adenocarcinoma. Cancer Res 2007; 67:11811–20.
24. Kanagavelu S, Gupta S, Wu X, Philip S, Wattenberg MM, Hodge JW, et al. In vivo effects of lattice radiation therapy on local and distant lung cancer: potential role of immunomodulation. Radiat Res 2014; 182:149–62.
25. Asur R, Butterworth KT, Penagaricano JA, Prise KM, Griffin RJ. High dose bystander effects in spatially fractionated radiation therapy. Cancer Lett 2015; 356:52–7.
26. Nolan MW, Gieger TL, Karakashian AA, Nikolova-Karakashian MN, Posner LP, Roback DM, et al. Outcomes of spatially fractionated radiotherapy (GRID) for bulky soft tissue sarcomas in a large animal model. Technol Cancer Res Treat 2017; 16:357–65.
27. Markovsky E, Budhu S, Samstein RM, Li H, Russell J, Zhang Z, et al. An antitumor immune response is evoked by partial-volume single-dose radiation in 2 murine models. Int J Radiat Oncol Biol Phys 2019; 103:697–708.
28. Filatenkov A, Baker J, Mueller AM, Kenkel J, Ahn GO, Dutt S, et al. Ablative tumor radiation can change the tumor immune cell microenvironment to induce durable complete remissions. Clin Cancer Res 2015; 21:3727–39.
29. Formenti SC, Demaria S. Systemic effects of local radiotherapy. Lancet Oncol 2009; 10:718–26.
30. Wennerberg E, Lhuillier C, Vanpouille-Box C, Pilones KA, Garcia-Martinez E, Rudqvist NP, et al. Barriers to radiation-induced in situ tumor vaccination. Front Immunol 2017; 8:229.
31. Chakravarty PK, Alfieri A, Thomas EK, Beri V, Tanaka KE, Vikram B, et al. Flt3-ligand administration after radiation therapy prolongs survival in a murine model of metastatic lung cancer. Cancer Res 1999; 59:6028–32.
32. Ahmed MM, Hodge JW, Guha C, Bernhard EJ, Vikram B, Coleman CN. Harnessing the potential of radiation-induced immune modulation for cancer therapy. Cancer Immunol Res 2013; 1:280–4.
33. Buchwald ZS, Wynne J, Nasti TH, Zhu S, Mourad WF, Yan W, et al. Radiation, immune checkpoint blockade and the abscopal effect: A critical review on timing, dose and fractionation. Front Oncol 2018; 8:612.
34. Rodriguez-Ruiz ME, Vanpouille-Box C, Melero I, Formenti SC, Demaria S. Immunological mechanisms responsible for radiation-induced abscopal effect. Trends Immunol 2018; 39:644–55.
35. Demaria S, Ng B, Devitt ML, Babb JS, Kawashima N, Liebes L, et al. Ionizing radiation inhibition of distant untreated tumors (abscopal effect) is immune mediated. Int J Radiat Oncol 2004; 58:862–70.
36. Demaria S, Kawashima N, Yang AM, Devitt ML, Babb JS, Allison JP, et al. Immune-mediated inhibition of metastases after treatment with local radiation and CTLA-4 blockade in a mouse model of breast cancer. Clin Cancer Res 2005; 11:728–34.
37. Hiniker SM, Chen DS, Knox SJ. Abscopal effect in a patient with melanoma. New Engl J Med 2012; 366:2035.
38. Postow MA, Callahan MK, Barker CA, Yamada Y, Yuan JD, Kitano S, et al. Immunologic correlates of the abscopal effect in a patient with melanoma. New Engl J Med 2012; 366:925–31.
39. Yamada Y, Bilsky MH, Lovelock DM, Venkatraman ES, Toner S, Johnson J, et al. High-dose, single-fraction image-guided intensity-modulated radiotherapy for metastatic spinal lesions. Int J Radiat Oncol Biol Phys 2008; 71:484–90.
40. Greco C, Zelefsky MJ, Lovelock M, Fuks Z, Hunt M, Rosenzweig K, et al. Predictors of local control after single-dose stereotactic image-guided intensity modulated radiotherapy for extracranial metastases. Int J Radiat Oncol Biol Phys 2011; 79:1151–7.
41. Savage T, Guha C. Radio-immunology of ablative radiation. In: Trifiletti D, Chao S, Sahgal A, Sheehan J, editors. Stereotactic radiosurgery and stereotactic body radiation therapy. Cham: Springer; 2019. p. 15–29.
42. Martinez-Zubiaurre I, Chalmers AJ, Hellevik T. Radiation-induced

transformation of immunoregulatory networks in the tumor stroma. Front Immunol 2018; 9:1679.

43. Kioi M, Vogel H, Schultz G, Hoffman RM, Harsh GR, Brown JM. Inhibition of vasculogenesis, but not angiogenesis, prevents the recurrence of glioblastoma after irradiation in mice. J Clin Invest 2010; 120:694–705.
44. Kozin SV, Kamoun WS, Huang Y, Dawson MR, Jain RK, Duda DG. Recruitment of myeloid but not endothelial precursor cells facilitates tumor regrowth after local irradiation. Cancer Res 2010; 70:5679–85.
45. Klug F, Prakash H, Huber PE, Seibel T, Bender N, Halama N, et al. Low-dose irradiation programs macrophage differentiation to an iNOSþ/M1 phenotype that orchestrates effective T cell immunotherapy. Cancer Cell 2013; 24:589–602.
46. Janiak MK, Wincenciak M, Cheda A, Nowosielska EM, Calabrese EJ. Cancer immunotherapy: how low-level ionizing radiation can play a key role. Cancer Immunol Immunother 2017; 66:819–32.
47. Liu R, Xiong S, Zhang L, Chu Y. Enhancement of antitumor immunity by low-dose total body irradiation is associated with selectively decreasing the proportion and number of T regulatory cells. Cell Mol Immunol 2010; 7:157.
48. Savage T, Pandey S, Guha C. Postablation modulation after single high-dose radiation therapy improves tumor control via enhanced immunomodulation. Clin Cancer Res 2020; 26:910–21.
49. Potiron VA, Abderrahmani R, Clement-Colmou K, Marionneau-Lambot S, Oullier T, Paris F, et al. Improved functionality of the vasculature during conventionally fractionated radiation therapy of prostate cancer. PLoS One 2013; 8:e84076.
50. Ministro A, de Oliveira P, Nunes RJ, dos Santos Rocha A, Correia A, Carvalho T, et al. Low-dose ionizing radiation induces therapeutic neovascularization in a pre-clinical model of hindlimb ischemia. Cardiovasc Res 2017; 113:783–94.
51. Mendonca MS, Chin-Sinex H, Dhaemers R, Mead LE, Yoder MC, Ingram DA. Differential mechanisms of x-ray-induced cell death in human endothelial progenitor cells isolated from cord blood and adults. Radiat Res 2011; 176:208–16.
52. Park HJ, Griffin RJ, Hui S, Levitt SH, Song CW. Radiation-induced vascular damage in tumors: implications of vascular damage in ablative hypofractionated radiotherapy (SBRT and SRS). Radiat Res 2012; 177:311–27.
53. Hellevik T, Martinez-Zubiaurre I. Radiotherapy and the tumor stroma: the importance of dose and fractionation. Front Oncol 2014; 4:1.
54. Chandra RA, Wilhite TJ, Balboni TA, Alexander BM, Spektor A, Ott PA, et al. A systematic evaluation of abscopal responses following radiotherapy in patients with metastatic melanoma treated with ipilimumab. Oncoimmunology 2015; 4:e1046028.
55. Kang J, Demaria S, Formenti S. Current clinical trials testing the combination of immunotherapy with radiotherapy. J Immunother Cancer 2016; 4:51.
56. Walshaw RC, Honeychurch J, Illidge TM. Stereotactic ablative radiotherapy and immunotherapy combinations: turning the future into systemic therapy? Br J Radiol 2016; 89:20160472.
57. Gay HA, Niemierko A. A free program for calculating EUD-based NTCP and TCP in external beam radiotherapy. Phys Med 2007; 23:115–25.
58. Wu Q, Mohan R, Niemierko A, Schmidt-Ullrich R. Optimization of intensity-modulated radiotherapy plans based on the equivalent uniform dose. Int J Radiat Oncol Biol Phys 2002; 52:224–35.
59. Amendola BE, Perez N, Amendola MA, Wu X, Ahmed MM, Iglesias AJ, et al. Lattice radiotherapy with RapidArc for treatment of gynecological tumors: Dosimetric and early clinical evaluations. Cureus 2010; 2:1–6.
60. Blanco Suarez JM, Amendola BE, Perez N, Amendola M, Wu X. The use of lattice radiation therapy (LRT) in the treatment of bulky tumors: A case report of a large metastatic mixed mullerian ovarian tumor. Cureus 2015; 7:e389.
61. Amendola BE, Perez NC, Wu X, Blanco Suarez JM, Lu JJ, Amendola M. Improved outcome of treating locally advanced lung cancer with the use of Lattice Radiotherapy (LRT): A case report. Clin Transl Radiat Oncol 2018; 9:68–71.
62. Amendola BE, Perez NC, Wu X, Amendola MA, Qureshi IZ. Safety and efficacy of Lattice radiotherapy in voluminous non-small cell lung cancer. Cureus 2019; 11:e4263.
63. Pollack A, Chinea FM, Bossart E, Kwon D, Abramowitz MC, Lynne C, et al. Phase I trial of MRI-guided prostate cancer lattice extreme ablative dose (LEAD) boost radiation therapy. Int J Radiat Oncol Biol Phys 2020; 107:305–15.
64. Bravin A, Olko P, Schultke E, Wilkens JJ. SYRA3 COST action–Microbeam radiation therapy: Roots and prospects. Phys Med 2015; 31:561–3.
65. Schultke E, Balosso J, Breslin T, Cavaletti G, Djonov V, Esteve F, et al. Microbeam radiation therapy – grid therapy and beyond: A clinical perspective. Br J Radiol 2017; 90:20170073.
66. Dilmanian FA, Krishnan S, McLaughlin WE, Lukaniec B, Baker JT, Ailawadi S, et al. Merging orthovoltage X-ray minibeams spare the proximal tissues while producing a solid beam at the target. Sci Rep 2019; 9:1198.
67. Tubin S, Khan MK, Salerno G, Mourad WF, Yan W, Jeremic B. Mono-institutional phase 2 study of innovative Stereotactic Body RadioTherapy targeting PArtial Tumor HYpoxic (SBRT-PATHY) clonogenic cells in unresectable bulky non-small cell lung cancer: profound non-targeted effects by sparing peri-tumoral immune microenvironment. Radiat Oncol 2019; 14:212.
68. Bodo S, Campagne C, Thin TH, Higginson DS, Vargas HA, Hua G, et al. Single-dose radiotherapy disables tumor cell homologous recombination via ischemia/reperfusion injury. J Clin Invest 2019 1; 129:786–801.
69. Greco C, Kolesnick R, Fuks Z. Conformal avoidance of normal organs at risk by perfusion-modulated dose sculpting in tumor single-dose radiation therapy. Int J Radiat Oncol Biol Phys 2020; Epub ahead of print.
70. Coleman CN, Ahmed MM. Implementation of new biology-based radiation therapy technology: When is it ready so ''Perfect makes practice?'' Int J Radiat Oncol Biol Phys 2019; 105:934–7.